

Design of Precursor Polymers Assists the Processing of Poly(ether ether ketone) Membranes in Solvents

Chi Zhang, Jiang-An You, Xue Wang, Rui Hou, Xiaofeng Li, Yuxuan Sun, Guorui Qin, Shenghai Li, and Suobo Zhang*



Cite This: *Macromolecules* 2024, 57, 2446–2457



Read Online

ACCESS |



Metrics & More

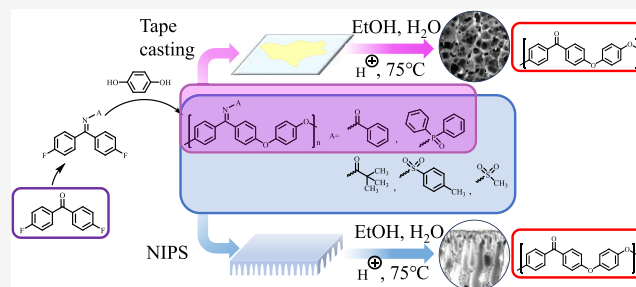


Article Recommendations



Supporting Information

ABSTRACT: By examining the structural patterns of the imine monomers engaged in polycondensation, a series of poly(ether ether ketone) precursor polymers (PEEKi-N-acyl) modified with N-acyl Imine groups were designed in this work. Contrary to poly(ether ether ketone) (PEEK), these precursor polymers have superior solubility, enabling their production in solution and processing of membrane components. The membrane components' substance could undergo an imine hydrolysis reaction in an acidic environment, turning them back into PEEK and giving them solvent resistance. In addition, the homogeneous polymer membranes of this series exhibit spontaneous pore formation under the action of ethanol, which was caused by solvent-induced internal stress relaxation. By utilizing the properties of this type of polymer, precursor polymers can be processed into PEEK sponge-like porous membranes, expanding the processing morphology and application range of PEEK.



INTRODUCTION

Poly(ether ether ketone) (PEEK), composed of phenyl ether and benzophenone units, is the most famous high-performance polymer (HPP) in the family of poly(aryl ether ketone)s. It can withstand high temperatures, chemical corrosion, complex organic solvents, mechanical abuse, and extreme weathering conditions while maintaining functional stability.^{1–9} This stability has sparked strong interest among researchers in the application of PEEK under extreme conditions. However, the high temperature resistance and organic environment tolerance of PEEK pose difficulties in its synthesis and processing, especially in membrane components with fine structures.^{10,11}

Solvent-resistant membrane separation technology is superior to distillation methods that rely on the phase transition in terms of energy savings. It can recover high-value-added products in organic solvents and achieve concentration, solvent exchange, and purification.^{12–14} The prerequisites for the application of separation membranes in organic solvents are functional stability, and solvent resistance. In addition, based on specific usage conditions, separation membranes require certain mechanical stability, high temperature resistance, acid resistance, etc.^{15–18} PEEK, a material with stable performance, fully meets functional requirements but is limited by its own stability in processing. For PEEK, good solvents only include concentrated sulfuric acid (98%) and methanesulfonic acid.^{19–21} The reason why these two solvents are not recommended in actual processing is not only due to their corrosiveness but also because: first, strong acid solutions can

cause sulfonation of PEEK molecular chains, thereby affecting the resistance of the membrane to solvents; second, strong acids make it challenging to use additives to alter the performance of membranes.²² That has led researchers to continuously seek new manufacturing methods for PEEK membranes.

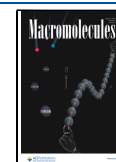
Researchers from Dow Chemical Company used high-boiling solvents and plasticizers to dissolve PEEK at high temperatures and spun them to prepare PEEK hollow fiber membranes.^{9,23,24} In addition, a mixture of molten PEEK and PEI can be employed to create membrane, and after that, PEI can be dissolved or broken down into small fragments by chemical reactions to etch the membrane's distinctive pore structure.^{25–27} Researchers have also sought alternatives to PEEK, such as sulfonated polyether ether ketone (SPEEK), which introduces functional groups that hinder the stacking of molecular chains in structural design, and poly(ether ether ketone) with cardo groups (PEEK-WC), which introduces relatively flexible sp³ hybridization sites in the molecular chain (Figure 1a,b).^{28–30} Despite every material being valuable, the solvent resistance of PEEK is sacrificed due to this structural alteration. Compared with this irreversible chemical modification and improvement, it is a more

Received: October 10, 2023

Revised: February 14, 2024

Accepted: February 16, 2024

Published: February 29, 2024



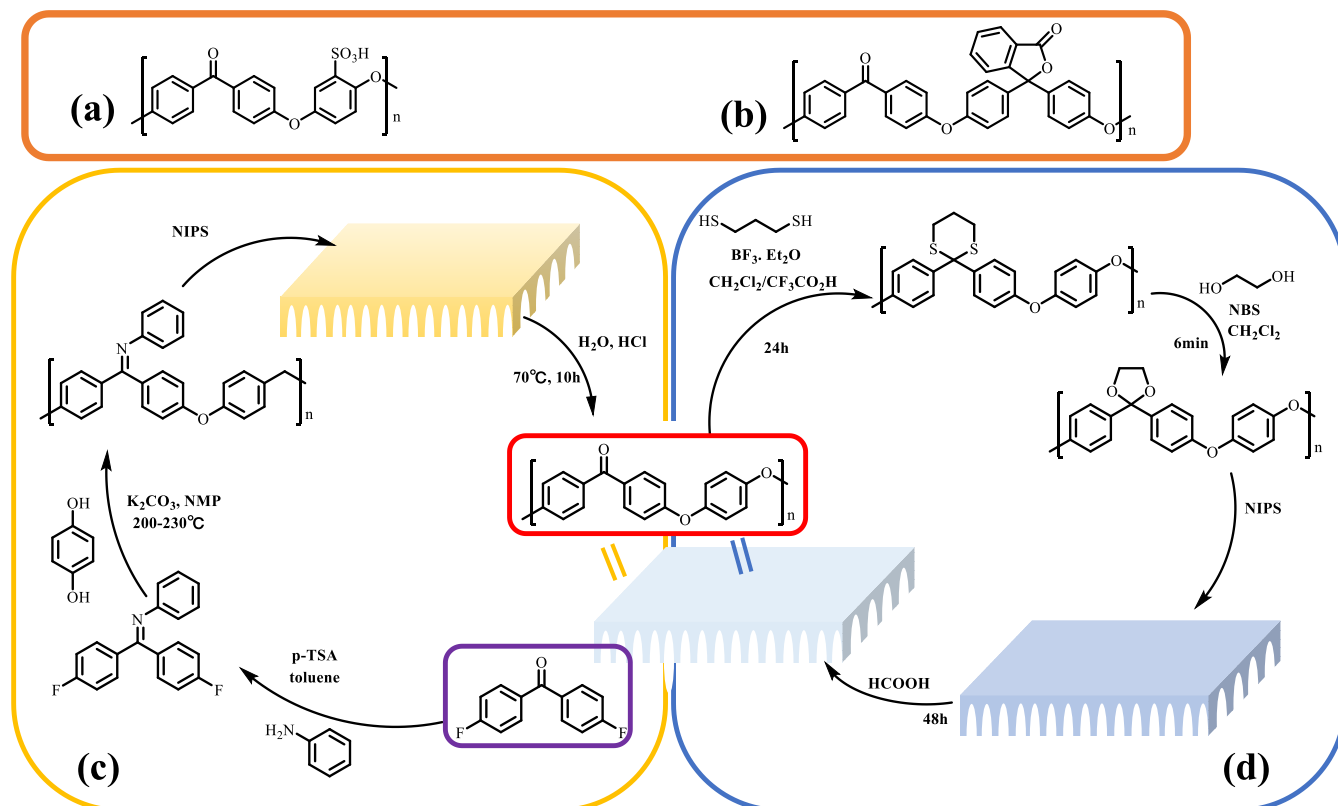


Figure 1. (a) Structural formula of SPEEK; (b) structural formula of PEEK-WC; (c) schematic diagram of the process of processing PEEK separation membranes by using PEEKt; (d) schematic diagram of the process of processing PEEK separation membranes by using ketal poly(phenylene ether).

useful idea to produce membranes using the precursor polymers of PEEK and then convert them to PEEK using chemical processes. Nunes³¹ et al. reported using ketal poly(phenylene ether) structures modified by dithioketone/ketal groups on the processing of PEEK membranes (Figure 1d). Although a strong acid solution is still required during the preparation of precursor polymers, the PEEK membrane prepared by this method can maintain the morphology formed by phase separation, is flexible, maintains constant permeability in tetrahydrofuran (THF), and is stable in *N,N*-dimethylformamide (DMF). The N-Ph group on the molecular chain of PEEKt also prevents the molecular chain from stacking, which results in solubilization of the polymer, as shown in Figure 1c. In contrast to SPEEK, the imine structure on PEEKt can be removed to restore the solvent resistance of PEEK without affecting the membrane morphology.^{32–35} The earliest application scenarios of this type of structure can be traced back to the work of McGrath et al.³⁶ in 1987. Subsequently, phenyl-substituted ketimines played an important role in the solubilization process of various insoluble polymers with ketone carbonyl groups.³⁷

The structural types of poly(aryl ether ketone) precursors reported so far include the ketal type and imine type. Compared to directly converting PEEK into ketal precursor polymers through dithioketone/ketal conversion, the introduction of imine structure requires starting with monomers, and imine monomers participate in the subsequent polycondensation process to achieve the preparation of the precursor polymers. Additionally, by introducing side groups at the monomer, it is possible to ameliorate the polymerization conditions. This strategy also makes it simpler to control the polymer's molecular weight.³⁵ Of course, this approach has drawbacks as well, such as the relatively poor imine monomer preparation efficiency, the

lengthy polycondensation time, and the lengthy hydrolysis time to transform PEEKt into PEEK. In order to improve the polycondensation activity of imine monomers and address the issue of slow imine hydrolysis rates on precursor polymers, a series of PEEK precursor polymers (PEEKi-N-acyl) have been produced in this study from the standpoint of structural design. The fabrication of PEEK membranes will be made exceptionally convenient by these precursor polymers. Meanwhile, the PEEKi-N-acyl series precursor polymer homogeneous membranes reported in this review exhibit unique stress relaxation phenomena under the influence of solvents, and the reasons for these phenomena are also analyzed.

EXPERIMENTAL SECTION

Materials. 4,4'-Difluorobenzophenone, hydroxylamine hydrochloride, 80% hydrazine hydrate solution, sodium acetate, triethylamine, diphenylphosphine chloride, lithium bis(trimethylsilyl) amide (LiHMDS), acetyl chloride, pentaerythritol chloride, benzoyl chloride, methanesulfonyl chloride, p-toluenesulfonyl chloride, hydroquinone, 2-aminobenzophenone, Sudan orange (SO), clonidine, para rosaniline (PB), methyl orange (MO), sunset yellow (SY), acidic fuchsin (AF), direct red 23 (DR23), and bengal rose red (RB) were purchased from Aladdin; 36.5–38% hydrochloric acid solution, dimethyl sulfoxide (DMSO), *N,N*-dimethylformamide (DMF), tetrahydrofuran (THF), sodium hydroxide (96%), petroleum ether, ethanol (EtOH), dichloromethane, *N,N*-dimethylacetamide (DMAc), trichloromethane (TCM), 1,2-dichloromethane (DCE), n-butanol (NBA), acetone (AC), toluene (PhMe), ethyl acetate (EtOAc), isopropanol (IPA), and acetonitrile (ACN) were purchased from Sinopharm.

Preparation of PEEK Asymmetric Membranes. The formula of the nanofiltration membranes' casting solution was precursor polymer PEEKi-N-Bz 23 wt % (the polymer can be found in the Results and Discussion), solvent 77 wt % (THF 30 wt %, DMAc 70 wt %). After standing and defoaming, the casting solutions were cast on a nonwoven

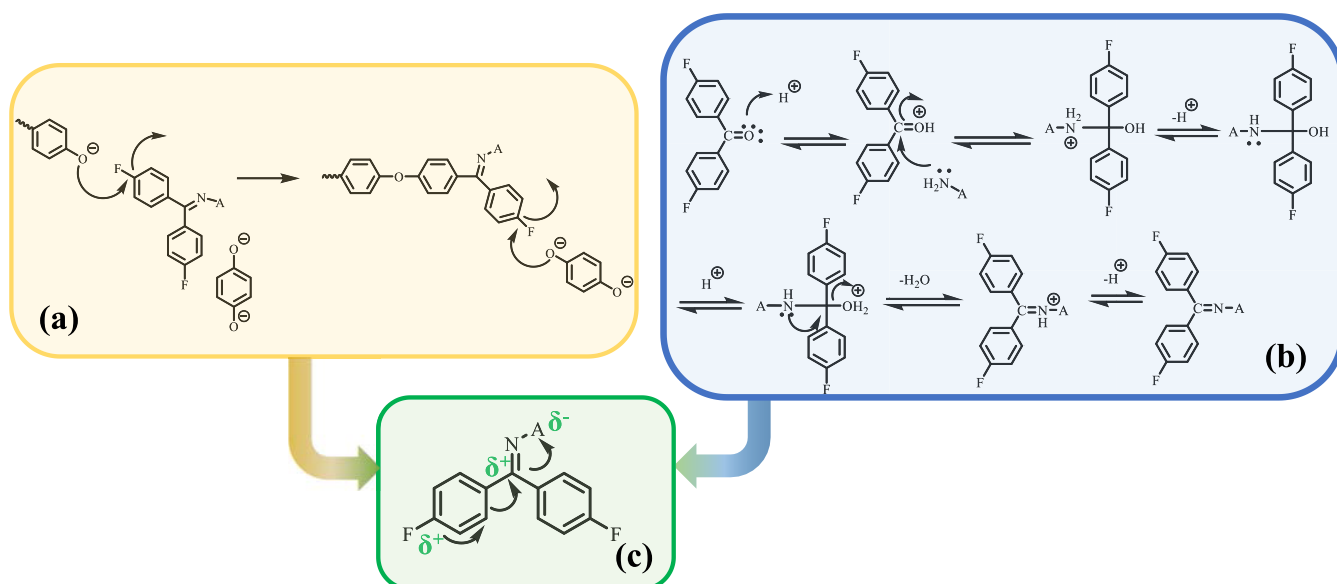


Figure 2. (a) Principle of polycondensation reaction; (b) formation and hydrolysis reaction mechanism of imines; (c) structural rules for imine monomers that can participate in the polycondensation reaction.

fabric (polyester fiber, 95 μm , 74.45 g/m^2) with a uniform-speed coating machine. The blade gap was 200 μm , the speed was 200 mm/s , the temperature was 30 $^\circ\text{C}$, and the humidity did not exceed 20%. The cast membranes were immediately immersed in water, and asymmetric membranes were prepared. PEEK asymmetric nanofiltration membranes were obtained by immersing the asymmetric membranes in 1 mol/L HCl at 75 $^\circ\text{C}$ for 2 h.

Preparation of PEEK Sponge Porous Membranes. After filtering and defoaming the 5 wt % PEEKi-N-phosphonyl/DMF solution (the polymer can be found in the [Results and Discussion](#)), a homogeneous film was prepared by casting it onto a horizontal glass plate in a 70 $^\circ\text{C}$ oven. After most of the solvents were removed, the membrane and glass plate were placed in a 70 $^\circ\text{C}$ vacuum oven for 24 h to remove residual solvents. Finally, a PEEKi-N-phosphonyl homogeneous membrane was prepared after peeling off the polymer layer on the glass plate ([Figure S22](#), TGA of polymer PEEKi-N-phosphonyl homogeneous membrane). The homogeneous membrane was placed in a solution of $\text{EtOH}/\text{H}_2\text{O} = 1:3$ at 75 $^\circ\text{C}$ for 1 h to obtain a sponge-like PEEKi-N-phosphonyl homogeneous membrane ([Supporting Information Video](#)). If 1 mol/L HCl was mixed into the solvent, the pore formation of the precursor polymer was accompanied by an imine hydrolysis reaction, resulting in a PEEK sponge porous membrane.

Characterization. The structure of monomers and polymers was confirmed by nuclear magnetic resonance hydrogen spectra (^1H NMR, AV300M). The surface and cross-sectional morphologies of homogeneous and porous membranes were characterized by SEM scanning (Merlin). The molecular weight of the polymer was measured by GPC (Cirrus Corporation, DMF).

The amine generated by the precursor polymer PEEKi-N-acyl undergoing imine hydrolysis under 1 mol/L HCl at 75 $^\circ\text{C}$ was detected by a UV spectrophotometer (Shimadzu), and the percentage of imine hydrolysis was measured by its absorbance change. The percentage of imine hydrolysis can be calculated by [eq 1](#):

$$\text{removal rate (\%)} = C_t/C_T \times 100\% \quad (1)$$

where C_t is the concentration of amine in the acidic solution at time t and C_T is the theoretical concentration of the side group solution after 100% hydrolysis of imine, which was calculated based on the mass percentage of side groups in the precursor polymer structure.

The viscosity of polymer solution was measured using a Ubbelohde viscometer (SYN THWARE), and the specific viscosity (η_{sp}) could be calculated by [eq 2](#):

$$\eta_{\text{sp}} = (\eta - \eta_0)/\eta_0 = t/t_0 - 1 \quad (2)$$

where η_0 is the viscosity of the pure solvent, η is the viscosity of the polymer solution, t is the time difference between the two scales of the Ubbelohde viscometer for the polymer solution, and t_0 is the time difference between the two scales of the Ubbelohde viscometer for the pure solvent.

Regarding the performance testing of solvent-resistant separation membranes, the formula for membrane rejection is given by [eq 3](#):

$$\text{rejection (\%)} = (1 - A_a)/A_0 \times 100\% \quad (3)$$

where A_0 is the absorbance of the original solution to be tested and A_a is the absorbance of the solution after membrane rejection.

The membrane permeance can be calculated by [eq 4](#):

$$\text{permeance (L m}^{-2} \text{ h}^{-1} \text{ bar}^{-1}) = \Delta m/(\rho \cdot S \cdot \Delta t \cdot P) \quad (4)$$

where $\Delta m/\rho$ is the permeate volume (L), S is the effective membrane area (m^2), Δt is the filtration time (h), and P is the operation pressure (bar).

The device for testing the membrane performance adopted a cross-flow mode. All results were the average of three tests.

RESULTS AND DISCUSSION

Design of Difluorophenylimine Monomers. Difluorinated N-A Imine structure that can participate in polycondensation can be obtained by iminizing the monomer 4,4'-difluorodibenzophenone. If the iminized product still has the ability to participate in polycondensation, then the following conditions must be met in terms of reactivity: First, as shown in [Figure 2a](#), each step of polycondensation involves an 'activated aromatic nucleophilic displacement (S_NAr)' reaction, where the carbon connected to the fluorine atom is nucleophilically attacked by the phenol monomer, completing the substitution reaction. Second, in order to produce PEEK that can withstand polar organic solvents, the precursor polymer must undergo hydrolysis of the imine structure on the main chain to ketone carbonyl groups in an acidic environment. As shown in [Figure 2b](#), the hydrolysis of imine satisfies the 'nucleophilic addition–elimination mechanism'. So as long as the imine structure designed meets the S_NAr reaction condition and the rules of

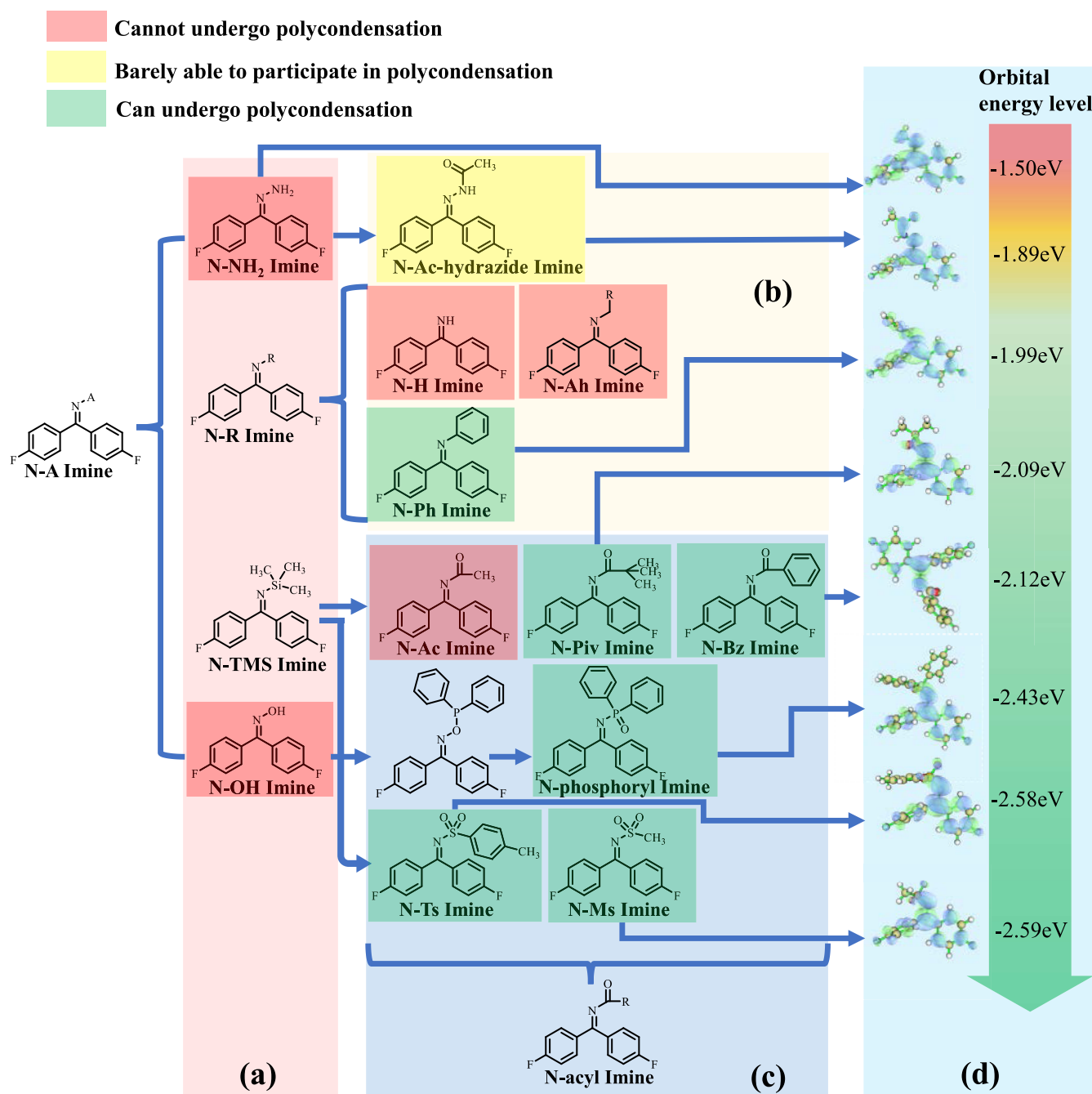


Figure 3. Ability of N-A Imine-derived structures to participate in polycondensation reactions. (a) The classical derivative structure of N-A Imine (N-NH₂ Imine, N-R Imine, N-OH Imine, and N-TMS Imine). (b) Derivative structures of N-NH₂ Imine (N-Ac-hydrazide Imine) and several types of N-R imines (N-H Imine, N-Ah Imine, and N-Ph Imine). (c) Structural modification of N-OH Imine and N-TMS Imine. (d) LUMO energy levels of imine monomers that can participate in polycondensation.

imine hydrolysis, in a sense, it has the possibility of being used for the synthesis of PEEK precursor polymer.

For the N-A Imine structure, the carbon linked to fluorine needs to be attacked by nucleophiles and participate in the polycondensation to form the polymer, while the imine on precursor polymers needs to be nucleophilically attacked by water molecules. According to the aforementioned research, if the substituent on N is an electron-withdrawing group, the imine-phenyl system's conjugation and induction effects will allow the N-A group to simultaneously reduce the electron cloud density of these two sites, as shown in Figure 2c, increasing the likelihood that these two sites will be attacked by

nucleophiles and allowing the monomer to meet the requirements for taking part in the synthesis of PEEK precursor polymers in terms of reactivity. When searching for suitable imine structures, classical imine structures and their derivatives could serve as structural frameworks (Figures S1–S10, the syntheses of several imine monomers), as shown in Figure 3.

The N-NH₂ Imine (Figure 3a), also known as the hydrazone structure, has been proven to have no polycondensation activity through actual polycondensation experiments. But the N-Ac-hydrazide Imine structure (Figure 3b) obtained by acylation of its amino group using acyl groups has just acquired the ability for polycondensation. Based on Figure 2c, it can be seen that the

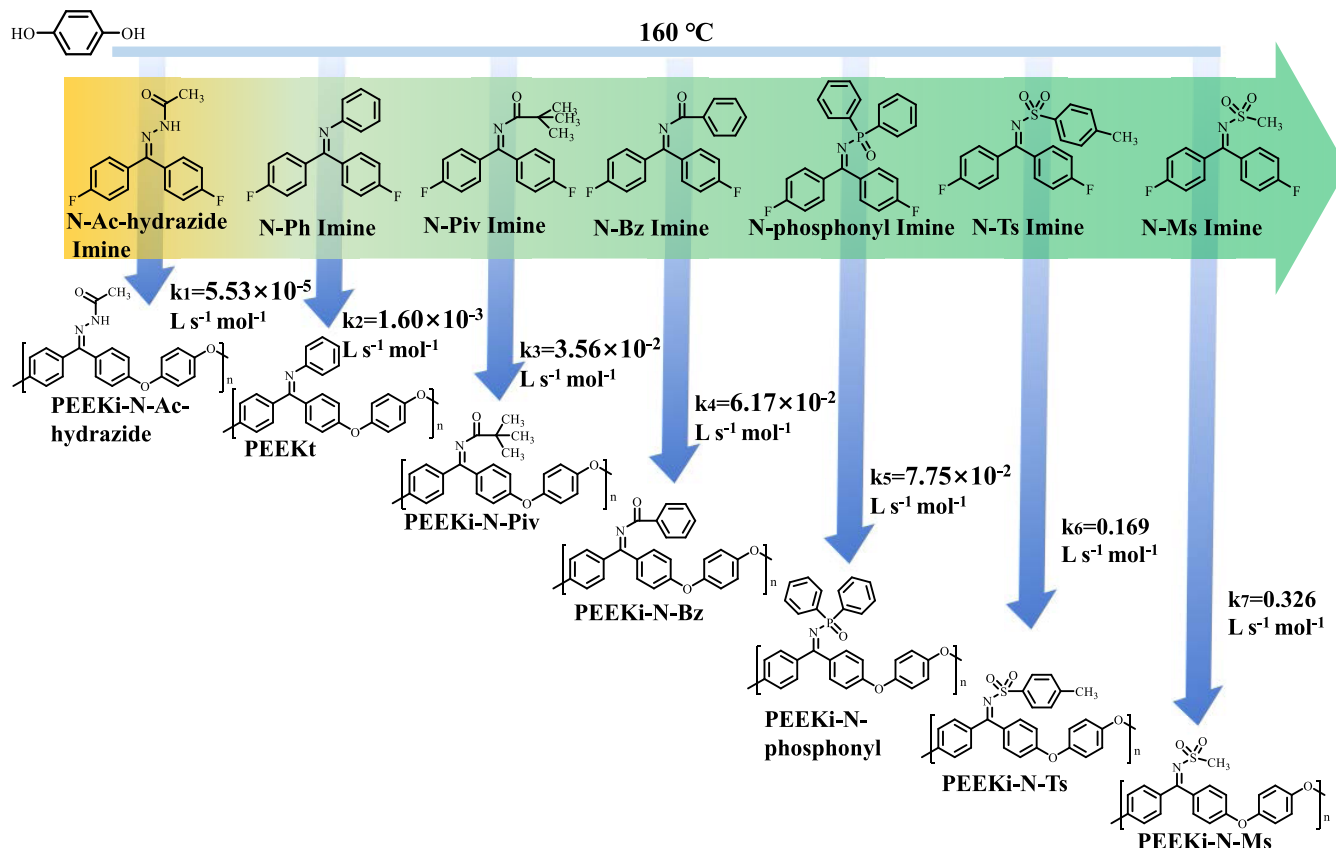


Figure 4. Rate constants of polymerization reactions of different imine monomers at 160 °C.

electron-donating ability of the amino group inhibits the substitution activity of nucleophilic substitution sites. The reaction activity of the substitution site of N-Ac-hydrazide Imine is enhanced by acylation, which weakens the electron-donating ability of the amino group. Several common types of N-R Imines include N-H Imine, N-Ah Imine, and N-Ph Imine, among which N-Ph Imine is the most classical structure. Compared with N-Ah Imine and N-H Imine, which cannot exist stably due to the large hydrolysis equilibrium constant,^{38–40} the conjugation effect between phenyl and imine enhances the overall stability of the structure. At the same time, phenyl is also a weak electron-withdrawing group, which meets the structural design in Figure 2c.

For the N-OH Imine structure, without going into its stability, hydrolysis potential, or nucleophilic substitution activity, the N-OH Imine structure is a three-functional structure due to the oxime hydroxyl group's inherent acidity, which prevents it from being a polycondensation monomer. However, oxime hydroxyl groups are easily modified sites. The conversion of the trivalent phosphate ester into the pentavalent phosphate ester, which results in a direct connection between the phosphonyl group and the hydrocarbon group, is a typical "Arbusov" rearrangement reaction in organic phosphate chemistry. This allows for the attempt to directly connect the imine and phosphonyl by introducing a trivalent phosphine structure into structural design.⁴¹ The trivalent phosphonate structure formed by the combination of the ketoxime structure and diphenylphosphine chloride can quickly rearrange into the structure of N-phosphonyl Imine (Figure 3c). As a member of the N-acyl Imines, the N-phosphonyl Imine can achieve both conjugated stable structure and electron-withdrawing effect

simultaneously. Furthermore, the phosphonyl group's ability to withdraw electrons from the structure is significantly better than that of the phenyl group.

Although the classical rearrangement reaction in phosphine chemistry is simple, this type of reaction can produce only phosphonyl groups. It is not feasible to construct more N-acyl Imine structures directly through imidization reactions, as these reactions also require the nucleophilicity of amines and the nucleophilicity of amides clearly does not meet the conditions. Therefore, N-TMS Imine can serve as an intermediate to construct more N-acyl Imine structures. As reported by Peterson et al.,⁴² N-TMS Imine was prepared by lithium di(trimethylsilyl) amide (LiHMDS) and 4,4'-difluorobenzophenone. Then, the TMS group of the structure could be replaced by an acyl group to achieve the acylation reaction of the imine.⁴³ Carbonyl and sulfonyl groups can be introduced into the imine structure in this way, resulting in structures including N-Ac Imine, N-Piv Imine, N-Bz Imine, N-Ts Imine, and N-Ms Imine (Figure 3c). Including the N-phosphonyl Imine obtained through rearrangement reactions, six N-acyl Imine structures are available.

After preliminary verification, except for the N-Ac Imine structure, which failed to polymerize, all other N-acyl Imine structures had excellent polymerization activity. It was verified that the acyl structure with α C-H will experience an intermolecular "aldol reaction", which will result in intermolecular bonding reactions of polymers and gel (Figures S18, analysis and verification of polycondensation failure of N-Ac Imine). After the α C-H groups are excluded, polycondensation can proceed normally, such as N-Piv Imine and N-Bz Imine (Figure 3c).

Polymerization Activity Testing of Imine Monomers.

By calculating the LUMO orbital energy levels, the reactivity of each monomer can be roughly predicted (Figure 3d); in particular, the reactivity of N-acyl Imines is higher than that of N-Ph imine.⁴⁴ In addition, based on the type of condensation reaction, the chemical reaction rate constants of each imine monomer under the same temperature and polymerization conditions can be calculated and compared to obtain more accurate conclusions about condensation activity (Figures S11–S17, the polycondensation process of imine monomers; Table S1, the calculation method of the polycondensation reaction rate constant). The calculation results are shown in Figure 4.

From these results, it can be seen that the polymerization activity of several N-acyl imines far exceeds that of N-Ph Imine, while the polymerization rate constant of N-Ac-hydrazide Imine, which has almost no polymerization ability, is lower than that of N-Ph Imine. These results are consistent with the order of the imine monomer reaction activity predicted by LUMO orbital energy levels.

The acylation of the N-NH₂ Imine structure achieves the polycondensation activity of the imine. However, after a long polymerization process at 160 °C for 13 h, the Mn of N-hydrazide imine with a polycondensation reaction rate constant (k_1) of $5.53 \times 10^{-5} \text{ L s}^{-1} \text{ mol}^{-1}$ only increased to 1237 g/mol (Figure S12c, the molecular weight of the polymer PEEKi-N-Ac-hydrazide). Different from the N-Ac-hydrazide Imine, the N-acyl Imine structures exhibited a much higher polycondensation activity than the N-Ph Imine structure. The effects of carbonyl and phosphonyl groups are not as strong as those of sulfonyl groups in the electron-withdrawing effect. Because of this, the N-Ts Imine structure could participate in polymerization at 130 °C and raise the product's Mn to 74441 g/mol within 15 min (Figure S16, preparation of polymer PEEKi-N-Ts), whereas the N-Ms Imine structure could start to polymerize at 100 °C (Figure S17, preparation of polymer PEEKi-N-Ms). Such polymerization activity is uncommon among halogenated polycondensation monomers. Due to their high polymerization activity, both types of imine monomers displayed a phenomenon that made it difficult to control the polymerization process, but the low-temperature polymerization ability of these structures also has unique value in special application environments.

Test of Imine Hydrolysis Ability of PEEK Precursor Polymers. In order to evaluate the hydrolysis ability of imine structures on several precursor polymers, the polymers PEEKi-N-Bz, PEEKi-N-phosphonyl, and PEEKi-N-Ts were selected for testing. (The amides generated by the hydrolysis of imines from these precursor polymers have aromatic rings, so the signal can be measured by UV spectrophotometry.) and compared with polymer PEEKt, the results are shown in Figure 5.

From the results shown in Figure 5, it can be seen that the side group hydrolysis rate of PEEKi-N-Bz and PEEKi-N-phosphonyl is very fast, and they can be hydrolyzed to over 90% in about 1 h in 1 mol/L HCl. Both polymers are more capable of hydrolyzing side groups than PEEKt. However, the imine hydrolysis ability of PEEKi-N-Ts seems to be even weaker than that of PEEKt. From the perspective of the imine being attacked by hydrophilicity, this result does not seem to fully comply with our expectations. Figure 2b makes clear that protonation is also necessary for the hydrolysis of imines in addition to nucleophilic attack. However, the alkalinity of the sulfonamides is too weak, which is obviously not conducive to protonation. The excessive electron-withdrawing effect really has a deleterious effect on

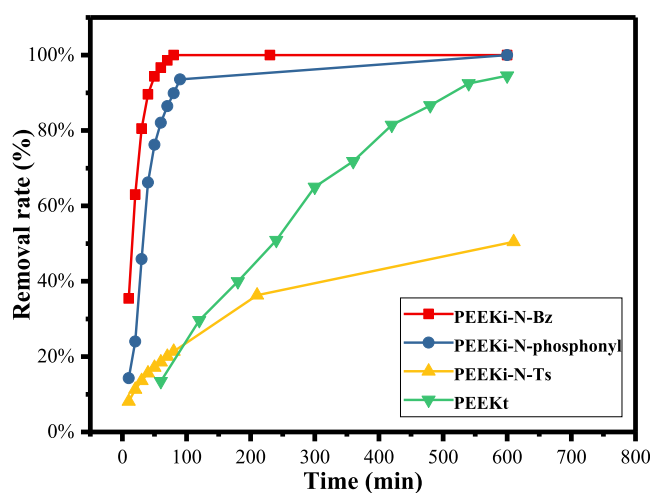


Figure 5. Changes in the imine hydrolysis percentage of several PEEK precursor polymers over time.

imine hydrolysis. Therefore, the structures that truly achieve both high polycondensation activity and a high imine hydrolysis rate are N-carbonimide and N-phosphoimide.

Performance of PEEK Solvent-Resistant Nanofiltration Membranes Prepared from PEEK Precursor Polymers.

The inclusion of substantial steric hindrance side groups results in the precursor polymers produced by N-acyl Imine structures having good solubility. By employing the nonsolvent-induced phase separation method (NIPS), the precursor polymers with a suitable molecular weight can be employed to prepare nanofiltration membranes. Finally, the side groups of the nanofiltration membrane can be removed under acidic conditions to produce the PEEK nanofiltration membrane. PEEK nanofiltration membranes were prepared from the polymer PEEKi-N-Bz (Figure S19, the morphology of the separation membrane made from precursor polymers before and after imine hydrolysis). The performance results of the nanofiltration membrane are shown in Figure 6.

As shown in Figure 6a,b,c, the PEEK solvent-resistant nanofiltration membrane prepared using the precursor polymer PEEKi-N-Bz has a molecular weight cutoff of 400 g/mol and can perform nanofiltration operations in various organic solvents, even withstanding strong polar nonproton solvents such as DMF, maintaining functional stability. The performance of this membrane is similar to that of the PEEK nanofiltration membrane made from PEEKt,³⁵ so polymer PEEKi-N-Bz can be used to prepare solvent-resistant membranes. Polymers PEEKi-N-Bz, PEEKi-N-Piv, and PEEKi-N-phosphonyl have obvious advantages in the rate of side group removal, and the prepared nanofiltration membranes are not inferior to traditional nanofiltration membranes in terms of permeance, rejection, and functional stability. Under the premise of ensuring the polymerization ability of imine monomers, as long as the imine side groups of the polymer are fully hydrolyzed, PEEK solvent-resistant nanofiltration membranes can be prepared. Therefore, several PEEK precursor polymers in this article all meet the requirements for membrane preparation under solution conditions.

Internal Stress Relaxation Phenomenon of the Polymer PEEKi-N-phosphonyl Homogeneous Membrane Affected by EtOH. The solubilization effect of the side groups of PEEK precursor polymers contributes to the solution-state processing of PEEK, providing convenience for

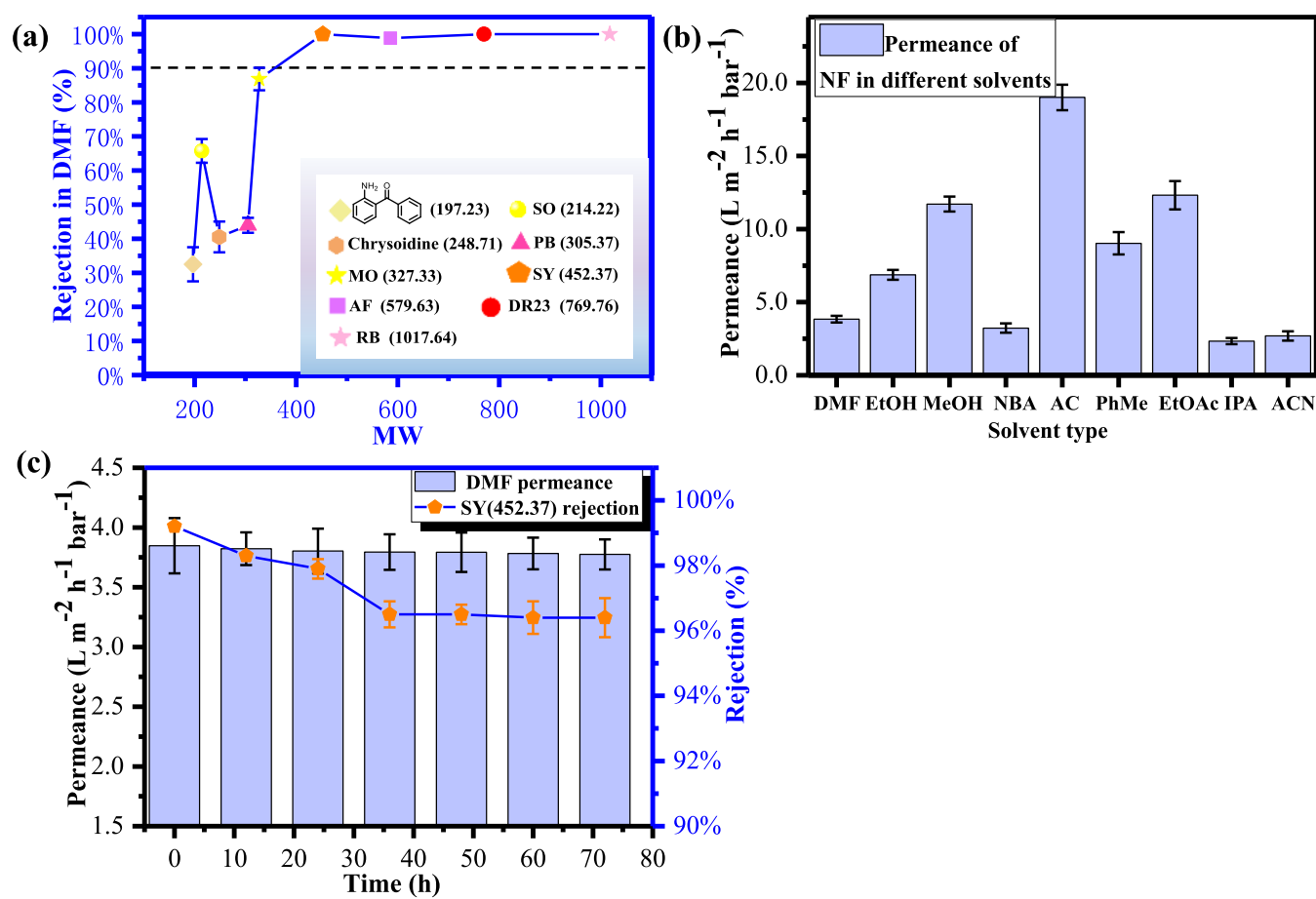


Figure 6. (a) Rejection of PEEK nanofiltration membrane in DMF; (b) permeance of PEEK nanofiltration membrane in different solvents; (c) long-term stability testing of PEEK nanofiltration membrane.

the process of processing PEEK asymmetric separation membranes. In addition to the basic solubilization effect, several PEEKi-N-acyl polymers also exhibit some properties different from those of classical PEEKt, as shown in Figure 7. When the homogeneous membrane of the polymer PEEKi-N-phosphonyl is immersed in a mixed solution of EtOH and H₂O at 1:3 at 75 °C, the macroscopic appearance of the polymer membrane will undergo a very significant change within a few minutes, and the membrane appearance will transform from a transparent homogeneous membrane to a white opaque membrane, as shown in Figure 7a,d (Figure S21 and Supporting Information Video, the specific process).

Through SEM testing results (Figure 7b,c,e,f), it can be seen that the “opacity” phenomenon corresponds to the appearance of sponge-like pores at the micro level, while the surface is still a relatively dense layer with some pores. This result is unexpected because it closely resembles the membrane’s shape as prepared by the phase separation method.⁴⁵ However, in this experiment, the appearance of sponge-like pores occurred in homogeneous membranes rather than polymer solutions, and this process does not involve any chemical reactions (Figure S22, the ¹H NMR of the membrane material before and after EtOH treatment). In related studies, the spontaneous physical morphology changes of thin films are associated with the effects of accumulated internal stresses in polymers.^{46,47} Residual stress is a common phenomenon in the processing of solid materials. Meanwhile, it has long been recognized that residual stress in glassy polymer films is an inevitable result of polymer deposition processes.⁴⁸

These residual stresses persist in the thin film, until sufficient annealing is performed to release the stress. When heated above glass-transition temperature (T_g), the stress gradually disappears as the molecular chains align to the equilibrium state.⁴⁹

It is difficult to quantify the internal stress present in amorphous polymers, so whether the pore-formation phenomenon is related to the internal stress in the polymer can be determined by controlling the conditions for the generation of internal stress. The experimental results are shown in Figure 8.

The pore-formation effect of the homogeneous membrane prepared under vacuum in Figure 8b is stronger than that of the homogeneous membrane in Figure 8a,c, because the rapid evaporation of solvent under vacuum conditions is conducive to the accumulation of internal stress and heating above the glass-transition temperature can eliminate internal stress in the polymer. From this, it can be seen that internal stress is one of the causes of the pore-formation phenomenon. The force fields of molecular chains on the surface of polymers are different from those within the bulk phase. The molecular chains at the material interface are more easily conformationally adjusted to eliminate internal stress, so the distribution of internal stress between the interface and the body of the homogeneous membrane is not consistent, which also explains why the obtained porous membrane is dense on both sides.

Experimental Testing of Solvent-Induced Internal Stress Relaxation. In the thin films by solvent-casting, residual stress can cause harmful effects, including the formation of microscopic defects and changes in macroscopic dimensions,⁵⁰

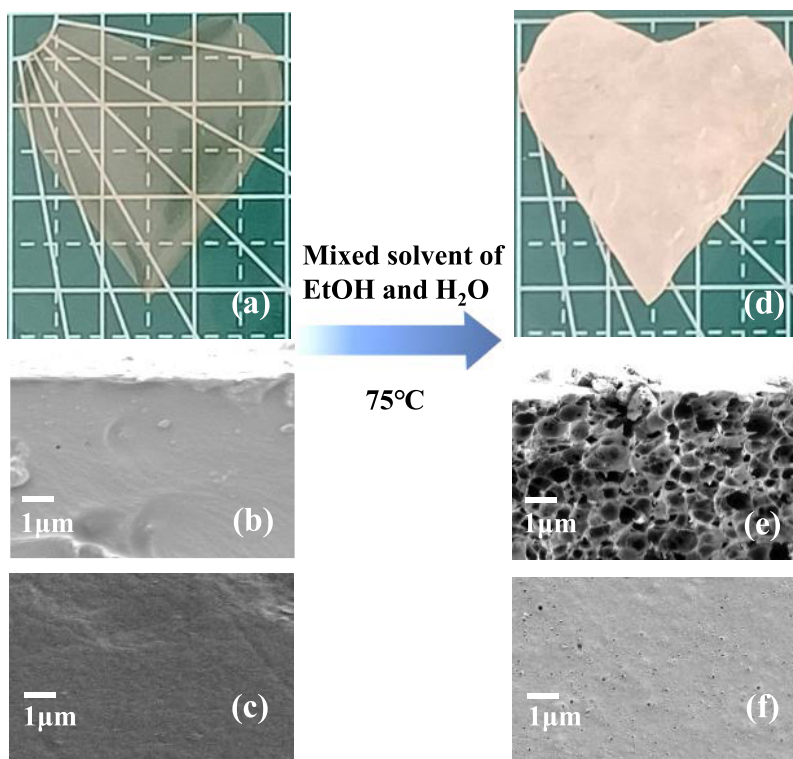


Figure 7. (a) Homogeneous membrane made from polymer PEEKi-N-phosphonyl; SEM scanning of PEEKi-N-phosphonyl homogeneous membrane: (b) cross section; (c) surface; (d) macroscopic morphology by immersing the PEEKi-N-phosphonyl homogeneous membrane in a mixture of alcohol and water ($\text{EtOH}/\text{H}_2\text{O} = 1:3$) at $75\text{ }^\circ\text{C}$ for 1 h; SEM scanning of PEEKi-N-phosphonyl porous membrane: (e) cross section; (f) surface.

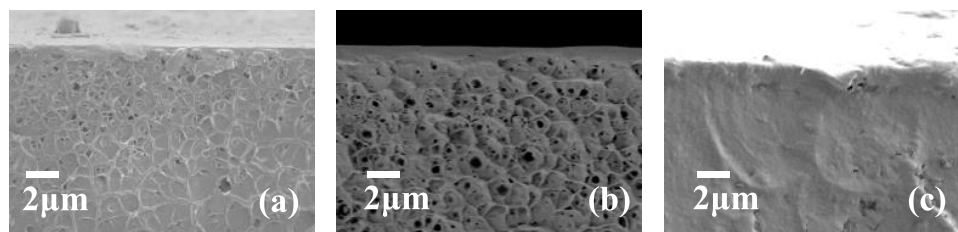


Figure 8. Cross-sectional morphology of the PEEKi-N-phosphonyl homogeneous membrane under different preparation conditions after soaking in a $75\text{ }^\circ\text{C}$ solution ($\text{EtOH}:\text{H}_2\text{O} = 1:3$) for 30 s. (a) Film formation by the flow casting method at atmospheric pressure at $50\text{ }^\circ\text{C}$. (b) Film formation by the flow casting method under vacuum at $50\text{ }^\circ\text{C}$. (c) Film formation by the flow casting method at atmospheric pressure at $120\text{ }^\circ\text{C}$.

which is different from the phenomenon in this experiment. The relaxation of internal stress in this experiment is achieved through EtOH. According to the report by Kotek et al.,⁵¹ porous fiber materials can be obtained by immersing electrospun nanofibers made from a mixture of nylon-6 solution and gallium trichloride (GaCl_3) in water, which is similar to the phenomenon observed in this experiment. In nylon solution, GaCl_3 was evenly spread; however, if only the salt were dissolved, such a pore size would not develop. This shows that during the soaking process in an aqueous solution, the salt and nylon phases separate, and the concentrated dissolution of the salt phase causes the development of such a vast volume of holes.⁵²

Dunn et al.⁵³ argued that this phenomenon was driven by internal stress and believed that the complexation between GaCl_3 and nylon would cause GaCl_3 to compete for hydrogen bonding sites between nylon molecules, thereby weakening the interaction between nylon molecules and making nylon easily affected by water. This effectively envelops the nylon molecular

chain with solvent molecules and leads to local plasticization and expansion of nylon, which leads to the movement of the nylon chains under internal stress and the formation of porous polymers. This also indicates that the solvent-induced internal stress relaxation phenomenon needs to consider not only the effect of internal stress but also the strength relationship between the interaction between solvent and molecular chains and the interaction between polymer molecular chains.

Cohesive energy density (ϵ) is a physical quantity used to evaluate the magnitude of the intermolecular forces. The solubility parameter (δ), which is equal to the square root of the cohesive energy density (ϵ), can be used to gauge a solvent's capacity to dissolve polymers, and it can also estimate the magnitude of the interaction between solvents and polymers. Assuming that the solubility parameters of the polymer are equal to those of a good solvent, the polymer fully unfolds in that solvent and has the highest viscosity. Therefore, the viscosity method can be used to explore the interaction relationship

between PEEKi-N-acyl series polymers and various solvents. The results are shown in Figure 9.

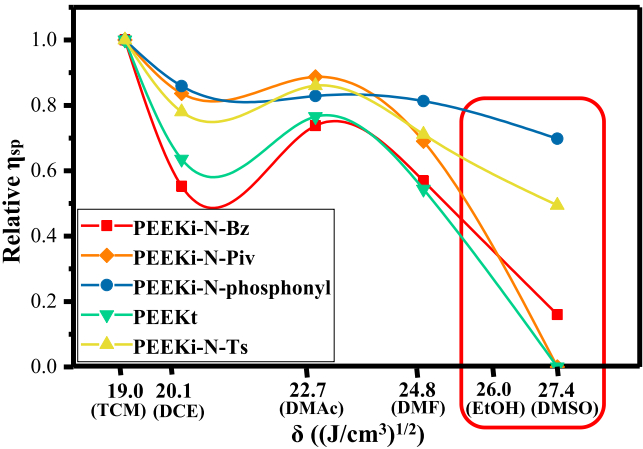


Figure 9. Changes in η_{sp} of polymers PEEKi-N-Bz, PEEKi-N-Piv, PEEKi-N-phosphonyl, PEEKt, and PEEKi-N-Ts in solvents with different solubility parameters.

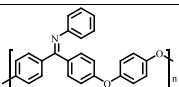

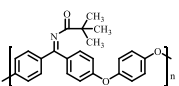
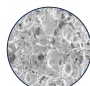
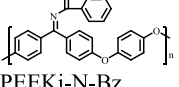
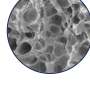
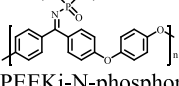
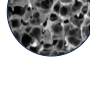
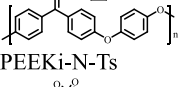
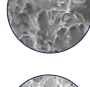
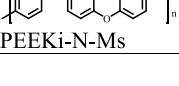

From Figure 9, it can be seen that the solubility parameters of several PEEK precursors are close to those of trichloromethane (TCM), which is $19 \text{ (J/cm}^3\text{)}^{1/2}$. The solubility parameter of EtOH is $26.0 \text{ (J/cm}^3\text{)}^{1/2}$, which is closest to the $27.4 \text{ (J/cm}^3\text{)}^{1/2}$ of DMSO. Therefore, to some extent, the more easily the polymer is dissolved by DMSO, the more susceptible it is to the influence of EtOH. The pore-morphology and pore-formation rate of different polymer homogeneous membranes vary, with the polymer PEEKi-N-phosphonyl having the fastest pore-formation rate and the densest pores (Table 1). From Figure 9, it

can be seen that PEEKi-N-phosphonyl is the most susceptible to the influence of EtOH. However, PEEKi-N-Piv and PEEKt, which have almost no pore-formation phenomenon, are completely insoluble in DMSO, indicating that they cannot be affected by EtOH easily. Therefore, the internal stress in the homogeneous membranes of PEEKi-N-Piv and PEEKt will not be relaxed due to the influence of EtOH.

The glass-transition temperature (T_g) is the lowest temperature at which polymer molecular chains move, which can be used to evaluate the strength of interactions between polymer molecules. The main chain structure of several polymers is the same; therefore, the difference is attributed to the structure of the A-groups, including factors such as polarity and volume. From Table 1, it can be seen that the T_g of several polymers and the pore-formation phenomenon. The polymers with excellent pore-formation ability include PEEKi-N-Bz and PEEKi-N-phosphonyl, with a T_g much lower than the $143 \text{ }^\circ\text{C}$ of PEEK, indicating weak intermolecular interactions. The T_g of PEEKi-N-Ts and PEEKi-N-Ms is higher, which may be attributed to excessive intermolecular interactions caused by polar sulfonyl groups. Although the viscosity test in Figure 9 shows that the polymers with the sulfonyl side group are strongly affected by EtOH, the pore formation is still weak because the interaction between ethanol and polymers cannot overcome the interaction between polymer molecular chains. As for PEEKi-N-Piv, although it has the lowest glass-transition temperature, it is not easily affected by EtOH to release internal stress and create pores due to the significant difference in solubility parameters compared with those of EtOH.

In summary, the results of viscosity testing and glass-transition temperature testing conform to the pore-forming law of PEEKi-N-acyl homogeneous membranes. It is determined that the pore-formation phenomenon of homogeneous membranes is

Table 1. Glass-Transition Temperature and the Pore-Formation Phenomenon of the Precursor Polymers

Polymer structure	Glass-transition temperature	The pores morphology
 PEEKt	150.0 $^\circ\text{C}$	
 PEEKi-N-Piv	77.6 $^\circ\text{C}$	
 PEEKi-N-Bz	83.5 $^\circ\text{C}$	
 PEEKi-N-phosphonyl	90.0 $^\circ\text{C}$	
 PEEKi-N-Ts	184.0 $^\circ\text{C}$	
 PEEKi-N-Ms	197.0 $^\circ\text{C}$	

influenced by internal stress, the interaction between solvents and polymer molecules, and the interaction between polymer molecules. The internal stress is related to the nonequilibrium conformational factors that control the molecular chain, such as the thermal history and aging value during the film-making process. The PEEK precursor polymer with large volume side groups creates favorable conditions for the accumulation of internal stress in homogeneous membranes, while the intermolecular and intramolecular interactions of the polymers depend entirely on the structure of the polymers themselves. Therefore, it can be seen that the phosphoimine side group of PEEKi-N-phosphonyl endows the precursor polymer with different processing characteristics under solvent conditions. Combining with the imine hydrolysis ability of the PEEKi-N-phosphonyl molecular chain, the sponge-like porous PEEKi-N-phosphonyl membrane obtained through internal stress relaxation can be transformed into a PEEK sponge porous membrane, greatly expanding the processing morphology of the PEEK membrane. A sponge-like porous PEEK membrane with excellent solvent resistance has the potential to be applied in fields such as lithium battery separators (Figures S23 and S24, performance testing of PEEK sponge-like porous membrane).

CONCLUSIONS

In this work, it was found that N-acyl imine structures with difluoro substitution can undergo polycondensation reactions with diphenol monomers to prepare precursor polymers through structural design and analysis of imine derivatives. The structures derived from N-acyl Imine include several monomers, such as N-Piv Imine, N-Bz Imine, N-phosphonyl Imine, N-Ts Imine, and N-Ms Imine, and the polycondensation activity of these N-acyl Imine structures far exceeds that of N-Ph Imine. The PEEKi-N-acyl precursor polymers prepared through this type of monomer not only have the same excellent solubility as PEEKt but also have advantages in the hydrolysis rate of polymer imine side groups. The solvent-resistant PEEK nanofiltration membrane made by hydrolysis of a PEEKi-N-Bz precursor membrane has a molecular weight cutoff of 400 g/mol and long-term functional stability. In addition, the solvent-induced internal stress relaxation law of the PEEKi-N-acyl series polymer homogeneous membranes was pointed out. Among these, the polymer PEEKi-N-phosphonyl homogeneous membrane can rapidly transform into a sponge-like porous membrane under the action of EtOH. Combined with the molecular chain imine hydrolysis property of this polymer, PEEK sponge-like porous membranes can be easily prepared. Therefore, the application of PEEKi-N-acyl series precursor polymers not only realizes the solution processing of PEEK but also expands the processing morphology of PEEK, broadening its application path.

ASSOCIATED CONTENT

Supporting Information

The Supporting Information is available free of charge at <https://pubs.acs.org/doi/10.1021/acs.macromol.3c02072>.

Preparation of imine monomers; polymerization of imine monomers and testing of polymerization reaction rate constants; morphology of the separation membrane made from precursor polymers before and after imine hydrolysis; TGA of polymer PEEKi-N-phosphonyl homogeneous membrane; summary of pore-formation phenomena in PEEKi-N-phosphonyl homogeneous

membrane; and performance testing of PEEK sponge-like porous membrane (PDF)

Internal stress relaxation phenomenon of the polymer PEEKi-N-phosphonyl homogeneous membrane affected by EtOH (MP4)

AUTHOR INFORMATION

Corresponding Author

Suobo Zhang — Key Laboratory of Polymer Ecomaterials, Changchun Institute of Applied Chemistry, Chinese Academy of Sciences, Changchun 130022, People's Republic of China; University of Science and Technology of China, Hefei 230026, People's Republic of China; orcid.org/0000-0002-1002-6197; Email: sbzhzhang@ciac.ac.cn

Authors

Chi Zhang — Key Laboratory of Polymer Ecomaterials, Changchun Institute of Applied Chemistry, Chinese Academy of Sciences, Changchun 130022, People's Republic of China; University of Science and Technology of China, Hefei 230026, People's Republic of China

Jiang-An You — Key Laboratory of Polymer Ecomaterials, Changchun Institute of Applied Chemistry, Chinese Academy of Sciences, Changchun 130022, People's Republic of China; University of Science and Technology of China, Hefei 230026, People's Republic of China

Xue Wang — Key Laboratory of Polymer Ecomaterials, Changchun Institute of Applied Chemistry, Chinese Academy of Sciences, Changchun 130022, People's Republic of China; University of Science and Technology of China, Hefei 230026, People's Republic of China

Rui Hou — Key Laboratory of Polymer Ecomaterials, Changchun Institute of Applied Chemistry, Chinese Academy of Sciences, Changchun 130022, People's Republic of China; University of Science and Technology of China, Hefei 230026, People's Republic of China

Xiaofeng Li — Key Laboratory of Polymer Ecomaterials, Changchun Institute of Applied Chemistry, Chinese Academy of Sciences, Changchun 130022, People's Republic of China; University of Science and Technology of China, Hefei 230026, People's Republic of China

Yuxuan Sun — Key Laboratory of Polymer Ecomaterials, Changchun Institute of Applied Chemistry, Chinese Academy of Sciences, Changchun 130022, People's Republic of China; University of Science and Technology of China, Hefei 230026, People's Republic of China

Guorui Qin — Key Laboratory of Polymer Ecomaterials, Changchun Institute of Applied Chemistry, Chinese Academy of Sciences, Changchun 130022, People's Republic of China; University of Science and Technology of China, Hefei 230026, People's Republic of China; orcid.org/0000-0002-6060-2658

Shenghai Li — Key Laboratory of Polymer Ecomaterials, Changchun Institute of Applied Chemistry, Chinese Academy of Sciences, Changchun 130022, People's Republic of China; University of Science and Technology of China, Hefei 230026, People's Republic of China

Complete contact information is available at:

<https://pubs.acs.org/doi/10.1021/acs.macromol.3c02072>

Notes

The authors declare no competing financial interest.

■ ACKNOWLEDGMENTS

This work was financially supported by National Natural Science Foundation of China (22378378, 52303141), the national key research and development program of China (2021YFB3801501), and Natural Science Foundation of Jilin Province (YDZJ202101ZYTS162).

■ REFERENCES

- (1) de Leon, A. C. C.; da Silva, I. G. M.; Pangilinan, K. D.; Chen, Q.; Caldona, E. B.; Advincula, R. C. High performance polymers for oil and gas applications. *React. Funct. Polym.* **2021**, *162*, No. 104878.
- (2) Hergenrother, P. M. The use, design, synthesis, and properties of high performance/high temperature polymers: an overview. *High Perform. Polym.* **2003**, *15*, 3–45.
- (3) Patel, P.; Hull, T. R.; McCabe, R. W.; Flath, D.; Grasmeder, J.; Percy, M. Mechanism of thermal decomposition of poly(ether ether ketone) (PEEK) from a review of decomposition studies. *Polym. Degrad. Stab.* **2010**, *95*, 709–718.
- (4) Manolakis, I.; Cross, P.; Colquhoun, H. M. Exchange Reactions of Poly(arylene ether ketone) Dithioketals with Aliphatic Diols: Formation and Deprotection of Poly(arylene ether ketal)s. *Macromolecules* **2017**, *50*, 9561–9568.
- (5) Shekar, R. I.; Kotresh, T. M.; Rao, P. M. D.; Kumar, K. Properties of High Modulus PEEK Yarns for Aerospace Applications. *J. Appl. Polym. Sci.* **2009**, *112*, 2497–2510.
- (6) Panayotov, I. V.; Orti, V.; Cuisinier, F.; Yachouh, J. Polyetheretherketone (PEEK) for Medical Applications. *J. Mater. Sci.: Mater. Med.* **2016**, *27*, No. 118.
- (7) Huang, T.; Li, J.; Chen, Y.; Zhong, T.; Liu, P. Improving permeability and antifouling performance of poly(ether ether ketone) membranes by photo-induced graft polymerization. *Mater. Today Commun.* **2020**, *23*, No. 100945.
- (8) Lan, P.; Meyer, J. L.; Vaezian, B.; Polycarpou, A. A. Advanced polymeric coatings for tilting pad bearings with application in the oil and gas industry. *Wear* **2016**, *354–355*, 10–20.
- (9) Xu, Q.; Wang, G.; Xiang, C.; Cong, X.; Gai, X.; Zhang, S.; Zhang, M.; Zhang, H.; Luan, J. Preparation of a novel poly(ether ether ketone) nonwoven filter and its application in harsh conditions for dust removal. *Sep. Purif. Technol.* **2020**, *253*, No. 117555.
- (10) Texier, A.; Davis, R. M.; Lyon, K. R.; Gungor, A.; McGrath, J. E.; Marand, H.; Riffle, J. S. Fabrication of PEEK/carbon fibre composites by aqueous suspension prepregging. *Polymer* **1993**, *34*, 896–906.
- (11) Wang, Z.; Guan, M.; Jiang, X.; Xiao, J.; Shao, Y.; Li, S.; Chen, Y. Bioinspired under liquid dual superlyophobic surface for on-demand oil/water separation. *Langmuir* **2023**, *39*, 870–877.
- (12) Marchetti, P.; Jimenez Solomon, M. F.; Szekeley, G.; Livingston, A. G. Molecular Separation with Organic Solvent Nanofiltration: A Critical Review. *Chem. Rev.* **2014**, *114*, 10735–10806.
- (13) Gould, R. M.; White, L. S.; Wildemuth, C. R. Membrane separation in solvent lube dewaxing. *Environ. Prog.* **2001**, *20*, 12–16.
- (14) Sereewatthanawut, I.; Baptista, I. I.; Boam, A. T.; Hodgson, A.; Livingston, A. G. Nanofiltration process for the nutritional enrichment and refining of rice bran oil. *J. Food Eng.* **2011**, *102*, 16–24.
- (15) Darvishmanesh, S.; Firoozpour, L.; Vanneste, J.; Luis, P.; Degreve, J.; Van der Bruggen, B. Performance of solvent resistant nanofiltration membranes for purification of residual solvent in the pharmaceutical industry: experiments and simulation. *Green Chem.* **2011**, *13*, 3476–3483.
- (16) Lively, R. P.; Sholl, D. S. From water to organics in membrane separations. *Nat. Mater.* **2017**, *16*, 276–279.
- (17) da Silva Bural, J.; Peeva, L.; Marchetti, P.; Livingston, A. Controlling molecular weight cut-off of PEEK nanofiltration membranes using a drying method. *J. Membr. Sci.* **2015**, *493*, 524–538.
- (18) Peeva, L.; Bural, J. S.; Vartak, S.; Livingston, A. G. Experimental strategies for increasing the catalyst turnover number in a continuous Heck coupling reaction. *J. Catal.* **2013**, *306*, 190–201.
- (19) Luan, J.; Zhang, S.; Zhang, M.; Geng, Z.; Wang, Y.; Wang, G. Preparation and characterization of high-performance poly(ether ether ketone) fibers with improved spinnability based on thermotropic liquid crystalline poly(aryl ether ketone) copolymer. *J. Appl. Polym. Sci.* **2013**, *130*, 1406–1414.
- (20) Huang, T.; Song, J.; He, S.; Li, T.; Li, X.-M.; He, T. Enabling sustainable green close-loop membrane lithium extraction by acid and solvent resistant poly(ether ether ketone) membrane. *J. Membr. Sci.* **2019**, *589*, No. 117273.
- (21) da Silva Bural, J.; Peeva, L.; Livingston, A. Towards improved membrane production: using low-toxicity solvents for the preparation of PEEK nanofiltration membranes. *Green Chem.* **2016**, *18*, 2374–2384.
- (22) Feng, X.; Peng, D.; Zhu, J.; Wang, Y.; Zhang, Y. Recent advances of loose nanofiltration membranes for dye/salt separation. *Sep. Purif. Technol.* **2022**, *285*, No. 120228.
- (23) Beck, H. N.; Lundgard, R. A.; Chau, C. C.; Wessling, R. A.; Mahoney, R. D. Film, fiber, and microporous membranes prepared from poly(etheretherketone) dissolved in high boiling point polar organic solvents. EP407684A1, 1991.
- (24) Sonnenschein, M. F. Improved spinnerette design for extrusion of polymeric large internal diameter hollow fiber membranes. *J. Appl. Polym. Sci.* **2002**, *83*, 2157–2163.
- (25) Ding, Y.; Bikson, B. Preparation and characterization of semi-crystalline poly(ether ether ketone) hollow fiber membranes. *J. Membr. Sci.* **2010**, *357*, 192–198.
- (26) Harris, J. E.; Robeson, L. M. Miscible blends of poly(aryl ether ketones) and poly(ether imides). *J. Appl. Polym. Sci.* **1988**, *35* (7), 1877–1891, DOI: 10.1002/app.1988.07035071.
- (27) Huang, T.; Chen, G.; He, Z.; Xu, J.; Liu, P. Pore structure and properties of poly(ether ether ketone) hollow fiber membranes: influence of solvent-induced crystallization during. *Polym. Int.* **2019**, *68*, 1874–1880.
- (28) Koch, T.; Ritter, H. Functionalized Poly(ether ether ketones) from 4,4-Bis(4-hydroxyphenyl)pentanoic Acid, 2,2'-Isopropylidenediphenol, and 4,4'-Difluorobenzophenone: Synthesis, Behavior, and Polymer Analogous Amidation of the Carboxylic Groups. *Macromolecules* **1995**, *28*, 4806–4809.
- (29) Cao, N.; Yue, C.; Lin, Z.; Li, W.; Zhang, H.; Pang, J.; Jiang, Z. Durable and chemical resistant ultra-permeable nanofiltration membrane for the separation of textile wastewater. *J. Hazard. Mater.* **2021**, *414*, No. 125489.
- (30) da Silva Bural, J.; Peeva, L. G.; Kumbharkar, S.; Livingston, A. Organic solvent resistant poly(ether-ether-ketone) nanofiltration membranes. *J. Membr. Sci.* **2015**, *479*, 105–116.
- (31) Aristizábal, S. L.; Chisca, S.; Pulido, B. A.; Nunes, S. P. Preparation of PEEK Membranes with Excellent Stability Using Common Organic Solvents. *Ind. Eng. Chem. Res.* **2020**, *59*, S218–S226.
- (32) Cao, N.; Sun, Y.; Wang, J.; Zhang, H.; Pang, J.; Jiang, Z. Strong acid- and solvent-resistant poly(ether ether ketone) separation membranes with adjustable pores. *Chem. Eng. J.* **2020**, *386*, No. 124086.
- (33) Feng, S.; Pang, J.; Yu, X.; Wang, G.; Manthiram, A. High-Performance Semicrystalline Poly(ether ketone)-Based Proton Exchange Membrane. *ACS Appl. Mater. Interfaces* **2017**, *9*, 24527–24537.
- (34) Lin, Z.; Cao, N.; Sun, Z.; Li, W.; Sun, Y.; Zhang, H.; Pang, J.; Jiang, Z. Based On Confined Polymerization: In Situ Synthesis of PANI/PEEK Composite Film in One-Step. *Adv. Sci.* **2022**, *9*, No. 2103706.
- (35) Sun, Y.; Zhou, S.; Qin, G.; Guo, J.; Zhang, Q.; Li, S.; Zhang, S. A chemical-induced crystallization strategy to fabricate poly(ether ether ketone) asymmetric membranes for organic solvent nanofiltration. *J. Membr. Sci.* **2021**, *620*, No. 118899, DOI: 10.1016/j.memsci.2020.118899.
- (36) Mohanty, D. K.; Lowery, R. C.; Lyle, G. D.; McGrath, J. E. Ketimine modifications as a route to novel amorphous and derived semicrystalline poly(arylene ether ketone) homo- and copolymers. *Int. SAMPE Symp. Exhib.* **1987**, *32*, 408–419.
- (37) Phillips, R. W.; Sheares, V. V.; Samulski, E. T.; DeSimone, J. M. Isomeric Poly(benzophenone)s: synthesis of Highly Crystalline Poly(4,4'-benzophenone) and Amorphous Poly(2,5-benzophenone),

a Soluble Poly(p-phenylene) Derivative. *Macromolecules* **1994**, *27*, 2354–2356.

(38) Shibata, S.; Masui, Y.; Onaka, M. Efficient solvent-free synthesis of N-unsubstituted ketimines from ketones and ammonia on porous solid acids. *Tetrahedron Lett.* **2021**, *67*, No. 152840.

(39) Kondo, Y.; Kadota, T.; Hirazawa, Y.; Morisaki, K.; Morimoto, H.; Ohshima, T. Scandium (III) Triflate Catalyzed Direct Synthesis of N-Unprotected Ketimines. *Org. Lett.* **2020**, *22*, 120–125.

(40) Sayer, J. M.; Conlon, Patrick. The timing of the proton-transfer process in carbonyl additions and related reactions. General-acid-catalyzed hydrolysis of imines and N-acylimines of benzophenone. *J. Am. Chem. Soc.* **1980**, *102*, 3592–3600.

(41) Hudson, R. F.; Brown, C.; Maron, A. The reaction between oximes and trivalent phosphorus compounds: a low-temperature radical rearrangement process. *Chem. Biochem. Eng.* **1982**, *115*, 2560–2573.

(42) Ager, D. J. The Peterson olefination reaction. *Org. React.* **1990**, *38*, 1–223.

(43) Georg, G. I.; Harriman, G. C. B.; Peterson, S. A. A Facile One-Flask Conversion of Aldehydes and Ketones to N-Sulfonyl Imines. *J. Org. Chem.* **1995**, *60*, 7366–7368.

(44) Lu, T.; Chen, F. Multiwfn: A multifunctional wavefunction analyzer. *J. Comput. Chem.* **2012**, *33*, 580–592.

(45) Jansen, J. C.; Macchione, M.; Oliviero, C.; Mendichi, R.; Ranieri, G. A.; Drioli, E. Rheological evaluation of the influence of polymer concentration and molar mass distribution on the formation and performance of asymmetric gas separation membranes prepared by dry phase inversion. *Polymer* **2005**, *46*, 11366–11379.

(46) Park, K. S.; Kwon, Y. D.; Kim, D. Theoretical and experimental analysis on the thickness-controlled residual stress during drying of solvent-absorbed polymer films. *Polym. J.* **2001**, *33*, 503–508.

(47) Thomas, K. R.; Steiner, U. Direct stress measurements in thin polymer films. *Soft Matter* **2011**, *7*, 7839–7842.

(48) Hu, S.; Wang, T.; Wei, T.; Peera, A.; Zhang, S.; Pujari, S.; Torkelson, J. M. Very low levels of n-butyl acrylate comonomer strongly affect residual stress relaxation in styrene/acrylic random copolymer films. *Polymer* **2022**, *260*, No. 125379.

(49) Gabriele, S.; Damman, P.; Sclavons, S.; Desprez, S.; Coppee, S.; Reiter, G.; Hamieh, M.; Al Akhrass, S.; Vilmin, T.; Raphael, E. Viscoelastic dewetting of constrained polymer thin films. *J. Polym. Sci.* **2006**, *44*, 3022–3030.

(50) Chung, J. Y.; Chastek, T. Q.; Fasolka, M. J.; Ro, H. W.; Stafford, C. M. Quantifying Residual Stress in Nanoscale Thin Polymer Films via Surface Wrinkling. *ACS Nano* **2009**, *3*, 844–852.

(51) Gupta, A.; Saquing, C. D.; Afshari, M.; Tonelli, A. E.; Khan, S. A.; Kotek, R. Porous nylon-6 fibers via a novel salt-induced electrospinning method. *Macromolecules* **2009**, *42*, 709–715.

(52) Dunn, P.; Sansom, G. F. Stress cracking of polyamides by metal salts. II. Mechanism of cracking. *J. Appl. Polym. Sci.* **1969**, *13*, 1657–1672.

(53) Dunn, P.; Sansom, G. F. Stress cracking of polyamides by metal salts. III. Mechanism of cracking. *J. Appl. Polym. Sci.* **1969**, *13*, 1673–1688.